On the prediction of shear brittle collapse mechanisms due to the infill-frame interaction in RC buildings under pushover analysis

On the prediction of shear brittle collapse mechanisms due to the infill-frame interaction in RC buildings under pushover analysis

Alessandra Fiore[1], Girolamo Spagnoletti[1] and Rita Greco[2]

[1]Technical University of Bari, DICAR, Via Orabona 4, 70125 Bari, Italy

[2]Technical University of Bari, DICATECh, Via Orabona 4, 70125 Bari, Italy

Corr. Auth. Alessandra Fiore, Technical University of Bari, Via Orabona 4, 70125 Bari, Italy, e-mail: a.fiore@poliba.it

ABSTRACT

A large number of research studies deal with the modeling and analysis of infilled reinforced concrete (RC) buildings under seismic actions, at the aim to understand the actual contribution given by masonry infills to the overall seismic resistance of a building. In this paper this aspect is investigated in the framework of pushover analyses, describing the theoretical and computational choices related to the involved parameters. Differently from the approaches available in literature and standards, the "double-strut model" is adopted to simulate the infill behavior, according to which an infill panel is represented by two equivalent non-parallel struts; the peculiarity is that the positions of the extremities of the two struts coincide with the points of application of the stress resultants on each side of the panel. The results show that, by adopting the double-strut model, it is possible to capture dangerous local shear failures which are usually neglected in pushover analysis and which can compromise the safety of the overall structure. By including in the analysis shear plastic hinges together with bending ones, it is evident how the additional shear forces, arising at the extremities of beams and columns, can substantially change the collapse mechanism of a structure under seismic action. The main features of the double-strut model are its low computational cost together with its accuracy, which make it particularly suitable for applications in the engineering practice. In fact it could be easily implemented in commercial calculation codes, representing a practical predictive tool able to enhance the safety level of infilled RC buildings.

Key words: reinforced concrete structure; infilled frame; double-strut model; shear brittle failure; collapse mechanism; pushover analysis.

1 INTRODUCTION

In Italy existing RC buildings are often characterized by the presence of infill panels which can interact with the primary structural elements under seismic action. A large number of research studies show that the presence of infilled panels in RC framed buildings can lead to conflicting effects on the structural response, depending on the mechanical properties, the geometrical distribution of infills and the interaction with the structural elements. Even if an increasing of structural stiffness and strength is expected, it is recognized that non-ductile damage mechanisms may be activated both at local (short column effect, brittle local failure, damages in joint region) and global scale (soft storey damage) [1-3].

With reference to a single frame, the increase in strength mentioned before is associated to an increase in the demand of shear capacity in some specific sections. Under lateral actions, the infill panel partially disconnects from the frame, remaining in contact with it only in correspondence of two opposite corners. RC frames (beams, columns and joints) can absorb the consequent increase of force, occurring in them due to their higher stiffness, only if they have sufficient shear overstrength. In the case of strong masonry infill, that is in the case of panels combined with frames having a low shear reinforcement, the activation of local brittle collapse mechanisms can become a major question and compromise the safety of the entire structure [4, 5]. Figure 1 shows the critical zones affected by the described local shear failure mechanisms due to the frame–infill interaction, while real case pictures can be found in [6].

This aspect of the frame-infill interaction constitutes the central issue of the present study, mainly referring for the previous considerations to existing buildings.

In the engineering practice, simplified macro-models approaches are often adopted to account for the influence of infills in structural analyses, also according to the specifications furnished by technical codes on this topic [7-9]. In particular the single equivalent strut method, based on the observation that the load path within the infill panel mainly follows the diagonal direction and introduced for the first time by Polyakov [10], is the most used one [11,12]. Such simplified approaches can be particularly appropriate in the cases when the goal is the evaluation of the global structural displacement demand; on the contrary they are not able to capture the possible influence of infills on load-bearing structural elements due to local effects, as a consequence of which unexpected brittle collapse mechanisms can occur under seismic action [13]. More complex macro-models adopt multiple parallel diagonal struts (two or three) in the attempt to reproduce these effects [14-17]. In particular, among the studies carried out on this regard, El-Dakhakhni *et al* [18]

introduced a three -strut model at the aim to reproduce a reliable distribution of bending and shear forces on the frame elements. Chrysostomou *et al* [19], in order to account also for the stiffness and strength degradation of infills, proposed a model with six compression inclined struts, i.e. three parallel struts for each diagonal direction, with the off-diagonal ones positioned at critical zones along the frame elements.

Liauw and Lee [20] investigated the efficacy of the diagonal strut model for masonry infills with and without openings, showing that the position of openings can significantly affect the strength and stiffness of panels.

Crisafulli and Carr [17] proposed a detailed multi-strut macro-model including both the classical diagonal truss elements and a special shear frictional strut aimed at reproducing the effect of vertical loads on the overall strength of the masonry infill. Recently the influence of vertical loads and openings has been further investigated by Campione *et al.* [21] and Asteris *et al.* [22].

Nevertheless the process of definition of the mechanical properties to attribute to the equivalent struts, as well as in which way taking into account the frame-infill stiffness ratios, are not clear yet, above all within nonlinear analyses [23-25].

The present paper focuses on the above aspects, underlining how a careful definition of the equivalent strut properties is of exceptional significance for achieving a realistic building response.

At this purpose two different panel macro-models are considered, the single equivalent strut model [11,12] and the double strut model proposed in [26], with the objective to point out how the collapse mechanisms can substantially change in the two configurations. Suitable nonlinear static analyses are thus carried out on a significant framed RC building, selected as case study and modeled in 3D, at the aim of appraising the influence of infill panels over the global and local collapse mechanisms under seismic action. In order to allow a critical comparison and deduce some observations about the infill modeling, three configurations are considered: the bare frame, the infilled frame and the frame with infills in correspondence of all storeys except for the first one (soft storey).

The theoretical and computational choices related to all the steps of the pushover analysis are accurately described in the paper. The final goal of the proposed study is in fact to provide a practical tool for the prediction of the real distribution of shear demand in frame critical sections when a macro-modeling approach is used within non linear static analyses. A first strategy in this direction is proposed in [6], where the local shear forces acting on beam and column ends is expressed as a fraction of the axial load experienced by the equivalent single strut. However the method, tested exclusively for specimens having two

different aspect ratios, could result rather onerous to be implemented in commercial calculation codes. In this framework the double-strut approach may represent an effective predictive tool for the accurate evaluation of frame-infill interaction effects in pushover analysis, since it could be easily implemented in commercial codes and could be applied for each dimension of panel frames. These topics are of crucial importance considering that the correct simulation of local brittle failures represents a major question in order to guarantee a proper safety level of infilled RC buildings.

2 MASONRY INFILL MODEL PARAMETERS

Based on the analytical and experimental studies carried out in the last decades, five different failure modes of masonry infilled frames can be recognized: Corner Crushing mode (CC mode), representing crushing of the infill in at least one of its loaded corners; Sliding Shear mode (SS mode), representing horizontal shear failure through bed joints at mid-height of a panel causing the cracking for sliding; Diagonal Compression mode (DC mode), representing crushing of the infill in the middle; Diagonal Cracking mode (DK mode), representing cracking across the compressed diagonal of the infill panel; Frame Failure mode (FF mode), in the form of plastic hinges in the columns or in the beam-column connection [14, 27].

Mixed collapse modes can also occur. It is worth noting that only the CC and SS modes are of practical interest. In fact the DC mode is very rare and can just occur in presence of a high slenderness ratio of the infill that could cause out-of plane buckling under in-plane loading. Similarly the DK mode and the FF have not particular interest since the first one does not represent a real failure mode, due to the circumstance that the panel still carries significant load after cracking, and the second one hardly occurs.

So the study herein carried out focuses on the CC mode, which first of all is coherent with the failure mode reproduced by both the single-strut model and the proposed double strut model [26] and also represents the most common modality of cracking of infills.

The fundamental parameters governing an equivalent strut model are: the number and position of struts; the width of the strut; the constitutive relationship of the panel, reproducing the failure mode. Due to the uncertainties and the extreme variability characterizing the mechanical properties of the infill, the definition of the above parameters presents some critical aspects that if not properly managed can compromise the reliability of the results.

The following sections provide some specific comments on the calibration of the panel macro-models to be used in pushover analyses.

2.1 Choice of the macro-model

In the research study herein presented two macro-models are adopted to simulate the behavior of infill panels: the single equivalent strut model (Fig. 2a) [11,12] and the double-strut model [26] (Fig. 2b).

According to the first approach, masonry elements are modeled as equivalent diagonal struts. This model has been supported by experimental laboratory tests, by observing that, under increasing loads, a panel-frame detachment happens at two opposite nodes while simultaneously the axial stress becomes relevant in the other two corners that are still in contact with the frame. The diagonal single-strut model requires a very low computational effort, but is affected by the impossibility to capture the local internal force distribution on RC members due to the interaction with infills. Nevertheless in practice it represents the most used strategy since it is able to properly reproduce the contribution to lateral stiffness given by infill panels at global level. It is also adopted by FEMA 356 code [7], that, differently from the Italian technical code [9] and Eurocode 8 [8], furnishes more specific indications on how to take infills into account in structural analysis.

The second approach was proposed in [26] in order to simulate the local interaction between panel and RC frame. It consists in adopting two equivalent non-parallel struts whose extremities coincide with the points of application of the stress resultants on each side of the panel. In order to furnish a practical tool, the positions of the extremities of the two equivalent struts were expressed in function of the dimensions of the panel. With reference to the first strut, the following expressions were obtained:

$$\begin{cases} \dfrac{d_1}{h} = 0.10834\left(\dfrac{l}{h}\right)^{-1} + 0.0073141\left(\dfrac{l}{h}\right)^{2} \\ \dfrac{b_1}{l} = 0.48689\left(\dfrac{l}{h}\right)^{-2} + 0.16302\left(\dfrac{l}{h}\right)^{0.5} \end{cases} \quad \text{for the first level;} \tag{1}$$

$$\begin{cases} \dfrac{d_1}{h} = 0.11609\left(\dfrac{l}{h}\right)^{-1} + 0.0061624\left(\dfrac{l}{h}\right)^{2} \\ \dfrac{b_1}{l} = 0.56509\left(\dfrac{l}{h}\right)^{-1} + 0.1287\left(\dfrac{l}{h}\right)^{0.5} \end{cases} \quad \text{for upper levels.} \tag{2}$$

Analogously the following expressions were obtained for the second strut:

$$\begin{cases} \dfrac{d_2}{h} = 0.157621\left(\dfrac{l}{h}\right)^{-1} + 0.084484\left(\dfrac{l}{h}\right)^{0.5} \\ \dfrac{b_2}{l} = 0.408621\left(\dfrac{l}{h}\right)^{-0.5} + 0.44431\left(\dfrac{l}{h}\right)^{0.5} \end{cases} \quad \text{for the first level;} \tag{3}$$

$$\begin{cases} \dfrac{d_2}{h} = 0.1025\left(\dfrac{l}{h}\right)^{-0.5} + 0.046736\left(\dfrac{l}{h}\right)^{0.5} e^{(l/h)^{-0.5}} \\ \dfrac{b_2}{l} = 0.312751\left(\dfrac{l}{h}\right)^{-1.5} + 0.467931\left(\dfrac{l}{h}\right)^{0.5} \end{cases} \quad \text{for the upper levels.} \tag{4}$$

The efficacy of the double strut model, already validated by literature experimental tests and investigated in linear field [26], is herein examined within the pushover analysis approach.

A wide literature can be found about the choice of the geometric characteristics of the struts, at the aim to achieve the equivalence in terms of strength and stiffness. The thickness of the strut is usually assumed as the same of the panel, whereas different proposals exist with reference to the width b_w. Theoretically, different values of the strut width should be adopted as loads increase, in order to take into account the progressive levels of degradation of the panel: b_w should be grater at the beginning, to represent the initial stiffness of the undamaged panel, and smaller in proximity of the failure, when only the central strip of the panel is still working. In the practice there are basically two main approaches. The first one defines b_w just as a function of the diagonal length of the panel. The formulations of Holmes [28], Paulay and Priestley [29], Penelis and Kappos [30] and some code provisions [31] belong to this first approach and are finalized to model just the initial linear elastic behavior of the panel, omitting the inelastic phase. The second one, more sophisticated, expresses b_w as a function of both the geometrical and mechanical properties of the panel and the adjacent frames. The formulations of Stafford and Smith [32], Klingner and Bertero [33], Bertoldi et al. [34], Papia et al. [35] belong to this second approach and refer to the inelastic phase, even if with different damage levels, so resulting particularly suitable for analyses in nonlinear field; nevertheless, due to the variability of the experimental conditions used to calibrate the above models, they lead to significantly different values of the parameter b_w, as it emerges observing Table 1 (for the properties of panels refer to Table 4).

In this study, in order to obtain physically consistent and comparable dimensions for the struts of both the used macro-models, the formulations proposed by Klingner and Bertero [3] (coinciding with FEMA provision) and Papia et al. [35] are adopted for the single-strut and the double-strut models respectively; in the second case the 50% of the widh b_w obtained by the Papia et al. formulation is assigned to each strut.

2.2 Choice of the constitutive model

A masonry infill strut model is commonly defined by an axial stress-strain relationship in the case of monotonic loading, and by the corresponding hysteretic rule in the case of cyclic loading, as well as by the

strength and stiffness properties, which as above stated are closely related to the evaluation of the equivalent strut width. Among the different force-displacement relationships available in literature to describe the mechanical behaviour of infill panels, the attention was focused on the models proposed by Panagiotakos and Fardis [36], Bertoldi et al. [34] and Cavaleri et al. [37].

In all cases the constitutive law is composed by four segments (Fig. 3): the first segment represents the initial shear behaviour of the uncracked panel; the second corresponds to the formation of the equivalent strut in the panel, after the detachment of the infill from the surrounding frame; the third describes the softening response of the panel after the critical displacement; the last one defines the final residual resistance of the panel.

Differently from the Panagiotakos and Fardis and Cavaleri et al. models which represent just the diagonal compression failure, the Bertoldi et al. formulation allows to represent four different collapse modes of the panel (Fig. 4a): crushing at the centre of the panel (DC mode); crushing of the corners (CC mode); sliding of the horizontal mortar joints (SS mode); diagonal failure (DK mode). The models regarding the last two collapse modes require the knowledge of mechanical parameters that are often difficult to identify, especially in the case of existing buildings, such as the shear resistance provided by the diagonal compression test, the sliding resistance of the bed joints or the average normal stress in the panel. By a sensitivity analysis carried out on panels with properties equal to the P_{X01} ones (see Table 4), it was also observed that the corresponding force values were so low to induce early collapse mechanisms in a pushover analysis, so under-estimating the strength of the overall structural system (Fig. 4a). Moreover, as already previously underlined, the DC and DK failure modes have a secondary relevance.

For this reason in the proposed study the Bertoldi et al. constitutive curve referring to the second failure mechanism was adopted, under the consideration that the CC mode can occur with the highest probability and it fully corresponds to the cracking mechanism on the basis of which the double strut model has been derived [26]. This constitutive model just depends on the compressive strength and the elastic moduli (longitudinal and tangential) of the masonry infill, in addition to the geometrical characteristics of the panel and the equivalent struts. More precisely, as it can be found in Bertoldi et al. [34], referring to Fig. 3, the main parameters to be defined in order to apply this constitutive law are K_m and F_m, which respectively represent the maximum strength and the stiffness of the equivalent strut.

The stiffness K_m is given by:

$$K_m = \frac{E_m b_w t_w}{d} \cos^2 \theta \tag{5}$$

where d, b_w and t_w are the diagonal length, the equivalent width and the thickness of the panel respectively, E_m is the mean Young modulus of masonry, θ is the slope of the infill diagonal.

In order to evaluate the maximum strength F_m, for the CC collapse mechanism, Bertoldi et al. [34] furnishes the following expression of the normal compressive ultimate stress σ_{w2} uniformly acting in the cross section of the equivalent strut:

$$\sigma_{w2} = \frac{1.12\sigma_{m0} \sin\theta \cos\theta}{K_1 (\lambda h)^{-0.12} + K_2 (\lambda h)^{0.88}} \tag{6}$$

where σ_{m0} is the average normal stress in the panel, h is the height of the panel and λ is the stiffness parameter, while the coefficients K_1 and K_2 are obtained by Table 2.

The parameter λ, expressing the relative stiffness of the panel with respect to the frame, can be determined as follows (Stafford and Smith):

$$\lambda = \sqrt[4]{\frac{E_w t_w \sin 2\theta}{4 E_C I_P h}} \tag{7}$$

where E_w and E_c are the elastic modulus of the infill panel and of the RC frame respectively, while I_P is the moment of inertia of the column.

The horizontal component of the corresponding critical force is given by:

$$F_m = \sigma_{w2} t_w b_w \cos\theta \tag{8}$$

According to Fig. 3, the resulting critical displacement is expressed by:

$$S_m = S_y + \frac{F_m - F_y}{K_2} \tag{9}$$

For example the values obtained for the panel P_{X01} (for the properties see Table 4), with reference to the single strut model, are reported in Fig. 4a; in this case, with reference to the CC collapse mechanism (σ_{w2}), it results: S_y=2.65 mm , S_m=13.25 mm , S_r=430.87 mm , F_y=276.9 kN , F_m=346.15 kN , F_r=121.15 kN (for the symbols see also Fig. 3).

As depicted in Fig. 4b, force values lower than the Panagiotakos and Fardis and Cavaleri et al. ones are so obtained, together with a larger displacement range.

It is worth noticing that, in the case of the proposed double strut model, in all the previous expressions involving the slope θ of the infill diagonal, for each strut its real inclination (θ_1, θ_2 in Fig. 2b) has been taken into account instead of θ. In the same way for each strut an elastic modulus coherent with its actual inclination has been considered instead of the diagonal one, as well as its effective length instead of d, together with its equivalent width b_w and thickness t_w. As to the elastic modulus, for each strut it has been calculated according to the following expression [27]:

$$E_\theta = \frac{1}{\frac{1}{E_0}\cos^4\theta + \left[-\frac{2\nu}{E_0} + \frac{1}{G}\right]\cos^2\theta\sin^2\theta + \frac{1}{E_{90}}\sin^4\theta} \tag{10}$$

where E_0 and E_{90} are the Young's moduli in the direction parallel and normal to the bed joints respectively; ν is the Poisson's ratio, defined as the ratio between the strain in the direction normal to the bed joints and the strain in the direction parallel to the bed joints; G is the shear modulus. Besides, the following relations have been achieved on the basis of experimental tests carried out for different typologies of masonries [6]: $E_0 \cong 0.75E_{90}$; $G \cong 0.4E_{90}$.

For sake of clearness it is also important to point out that the constitutive law proposed by Bertoldi et al. [34] was obtained by analyzing the seismic behavior of 10 different frames characterized by two equal-span bays and a varying number of equal-height storeys (from 2 to 24). The approach proposed in [34] is surely more related to the mechanic of the system with respect to others available in literature since all the main possible failure modalities are taken into account, but a large validation including the most used typologies of infill is missing and should be implemented in order to assess the actual applicability of the constitutive law.

3 THE CASE STUDY

The case study is represented by a 4-storeys RC framed building, symmetric in both longitudinal and transversal directions; it consists of five bays in the x-direction and three bays in the y-direction. The building is regular both in plan (with two symmetry axes in the x and y directions) and in elevations (no variations in masses or stiffness are present). The in plan dimensions are 25.3 m x 17.85 m and the interstorey height is 3.5 m for all levels except for the ground floor, that is 4.3 m high (Fig. 5).

In all storeys beams are 30 cm wide and 60 cm high (Fig. 6a), while columns are 30x80 cm^2 except for the angular ones that are 30 x 60 cm^2 (Fig. 6b). Floors have a mixed structure made up by cast-in-place concrete

and hollow tile bricks, for a total thickness of 30 cm (Fig. 6c). Infill panels are included along the outside frames, are made of hollow bricks and are 36 cm thick. Mechanical parameters of reinforced concrete and infill panels are summarized in Tables 3 and 4 respectively. Floor diaphragms are considered rigid in their own plane and the structure is assumed perfectly constrained at the basis. On this topic it is worth to note that, according to Eurocode 8 [8], a floor diaphragm may be considered as rigid if: *i*) when it is modelled with its actual in-plane flexibility, under seismic load condition, its horizontal displacements do not exceed anywhere by more than 10% the corresponding ones that would result from a rigid diaphragm assumption; *ii*) its thickness and reinforcement (in both horizontal directions) are above the minimum value of 70 mm and the minimum slab reinforcement as prescribed by Eurocode 2 [38], respectively. It should also be considered that a diaphragm, in order to be considered as rigid, should be free of large openings, especially in proximity of the main vertical structural elements [39].

The structure is modeled by using the FE analysis program SAP2000. Five models are overall taken into account: Mod A, bare structure (Fig. 7a); Mod B.1, structure with infills modeled as a single-strut in all storeys; Mod B.2, structure with infills modeled as a double-strut in all storeys (Fig. 7b); Mod C.1, structure with infills modeled as a single-strut in all storeys except for the first one which is bare (Fig. 7c); Mod C.2, structure with infills modeled as a double-strut in all storeys except for the first one which is bare.

3.1 Characterization of the pushover analysis parameters

The seismic behavior of the five models is investigated in non-linear field by performing suitable non-linear static procedures [40]. The non-linear static analysis exploits two different computational models of the structure: a multi-degree-of-freedom (MDOF) model, on which a ‘‘pushover’’ numerical analysis is performed, and an ‘‘equivalent’’ single-degree-of-freedom (SDOF) system, derived from the previous one after proper manipulations, devoted at the analysis by the design response spectrum.

Pushover analysis is a non-linear procedure carried out under conditions of constant gravity loads and increasing horizontal loads [8, 9, 41]. The values of the latter are increased monotonically step by step, until a failure mechanism is achieved. Two different lateral load distributions are herein used: a “uniform” pattern (2a), with a force applied at each node proportional to the mass tributary to that node; a “modal” pattern (1b), with a force applied at each node proportional to the product of the displacement of the node in the first mode shape times the mass. A vertical load equal to $G_k + 0.3Q_k$ is introduced at step 0 and then kept

unchanged during the analysis. Separate 3D pushover analyses are performed in the two horizontal directions.

Each RC building is treated as a frame element model, in which the spread of inelasticity is implemented through the formation of non-linear plastic hinges at the frame element's ends during the incremental loading process. Pure moments hinges and axial-moment hinges are assigned to the two ends of beams and columns respectively. The moment-rotation relationship of a plastic hinge is modelled as a trilinear curve constituted by the elastic, hardening and softening segments (Fig. 8a) [41, 42].

The non linear behaviour of masonry panels is described according to the Bertoldi et al. constitutive curve (second failure mechanism), as specified in Section 2 (Fig. 8b).

For each analysis the capacity curve, i.e. the plot of the base shear force versus the displacement of the control point (middle point at the top of the building), is computed; it is representative of the resistance of the structure when deforming into the inelastic range. Each pushover analysis is carried out under displacement control and, according to SAP2000 software, it stops when one of the following circumstances occurs: *i*) the displacement of the control point reaches a pre-defined value (herein set equal to 1000 mm); a sufficient number of plastic hinges form and the system reaches a plastic mechanism, so that the iterative procedure cannot converge.

The non-linear static analysis is based on the assumption that the response of the structure can be related to the response of an equivalent SDOF system. Accordingly, after each pushover curve of the actual MDOF structure is obtained, it is scaled by the transformation factor Γ [8] and converted into an equivalent SDOF bilinear curve by using an energy based approach. The elastic period T^* of the idealised elastic-perfectly plastic SDOF model is so derived; the displacement demand (target displacement) of the structure with period T^* associated to the seismic performance level under consideration can be estimated through the elastic response spectrum at the period T^*. Finally for the required hazard intensity the seismic performance of the structure is assessed by transforming back the displacement demand from the SDOF system to the MDOF one and by comparing the seismic demand with the capacity.

Seismic hazard parameters of the site for the three performance levels of Near Collapse (NC), Significant Damage (SD) and Damage Limitation (DL) are summarized in Table 5.

According to the codes in force [8, 9], the local ductility and deformation demands from pushover analysis should not exceed the corresponding capacities which implies that brittle elements should remain in elastic

field. To ensure this, suitable local verifications are required, by checking for each element the demands in terms of rotations or shear forces in correspondence of the pushover step nearest to the target displacement of the selected limit state.

The attention is here addressed to the shear failure mechanisms, that is for each element it should be verified that, at the pushover step in correspondence of the target displacement, the acting shear force is lower than the shear resistance V_{Rd}.

In order to investigate this particular topic, also pushover analyses including shear hinges at the nodal end sections of columns and beams in contact with infill panels, in addition to moments/axial-moments ones, are properly performed. Coherently with the above assumption, for the shear hinge the rectangular force-displacement law depicted in Fig. 8c is considered, where the limit shear value is assumed equal to the shear resistance V_{Rd}. In accordance to Eurocode 2 [38], the shear resistance V_{Rd} is calculated as the smallest value between the design value of the shear force which can be sustained by the yielding shear reinforcement $V_{Rd,s}$ and the design value of the maximum shear force which can be sustained by the member limited by the crushing of the compression struts $V_{Rd,max}$. In the same force-displacement diagram, recalling the deformed configuration of RC frames under seismic action, for the columns the maximum displacement is assumed equal to the product $\theta_u h$, θ_u being the ultimate rotation and h being the storey height. In this way it is assumed that the value of $\tan\theta_u$ is similar to θ_u. The rotations θ_u corresponding to the ultimate condition are evaluated by adopting the equation contained in the Italian seismic code [9] which is in complete agreement with Eurocode 8. Displacement values comparable to the maximum allowable interstorey drift according to Eurocode 8, that is to $0.005h$, are so obtained. Conversely in the case of beams, for the maximum displacement, a smaller value, near to zero, is considered; in fact beams are not subjected to significant vertical displacements and anyway shear forces are smaller than column ones, so it is improbable that shear cracking earlier occurs in beams.

4 ANALYSIS RESULTS

For each model a modal analysis was firstly carried out, at the aim to assess the dynamic behavior of the structure. It was found that the first two modal shapes are the translational ones (in the x and y directions), both in the case of the bare and infilled models, with high modal participating ratios, as it is typical of regular buildings. As expected, the modes of vibration in the y direction, corresponding to the shorter and then

weakest side of the building plan, are characterized by higher periods than the ones in the *x* direction. Figure 9 shows for each model the values of the natural vibration periods associated to the first six mode shapes. A period reduction can be observed moving from the bare structure (Mod. A) to the models with infill panels and soft storey (Mod. C.1 and C.2), as well as a further period reduction can be observed moving to the models where all infills are present (Mod. B.1 and B.2). These results confirm how the presence of infill panels produce an increment in the structural stiffness and thus a reduction of the natural vibration periods, more remarkable in absence of soft storey. It should be also observed that the choice of the panel macro-model does not significantly affect the natural modes of vibration, proving the equivalence at global level of the double and single strut models.

In non linear field, numerical analyses were firstly aimed at investigating the influence of the elastic properties of the infill, in terms of elastic moduli, on the pushover results. Figure 10a shows the capacity curves obtained by adopting different values of the infill elastic modulus in the Bertoldi et al. constitutive curve, with reference to model B.2, force distribution 1b) and *x* direction. By increasing the value of the elastic modulus, the characteristic forces slightly modify, while the corresponding displacements significantly decrease since the stiffness of the softening, elastic and yield branches of the constitutive law modifies (Fig. 10b). In fact as the value of the elastic modulus increases as well the stiffness of the equivalent struts increases too. From a numerical standpoint, an early interruption of the analysis occurs at higher values of the infill elastic modulus, due to clear convergence problems. As a consequence the values E_0=825 MPa and E_{90}=1100 MPa, consistent with clay hollow bricks [43], were adopted in the pushover analyses.

Figures 11a,b show for each direction the capacity curves of all models with reference to the 1b) force pattern. As already pointed out for the modal analysis, the results confirm that including the contribution of infills in the RC frame induces a significant increase of the stiffness and strength of the overall structure. Within the models with infills, the lateral stiffness of the structures modeled by adopting the double-strut approach is slightly higher with respect to the ones obtained by the single-strut model. This result can be observed in Table 6 where the global stiffness percentage-increments of infilled structures with respect to the bare model are summarized in function of the force direction, the load pattern and the infill panel macro-model.

By comparing the seismic demands with the capacities for the relevant performance levels of NC, SD and DL, it also emerges that, in accordance to the previous statements dealing with the global response, the single-strut and the double-strut models provide similar and comparable results (Figs. 11a, b). Moreover it should be observed that the percentage ratios between the displacement associated to the maximum base shear and the one corresponding to the NC condition decrease moving from the bare structure (Mod. A) to the models with infills in all storeys (Mod. B.1 and B.2) and increase moving from the bare structure (Mod. A) to the models with infills and soft storey (Mod. C.1 and C.2), in correspondence of which reach the maximum values. From this behaviour it can be deduced that the presence of infills in all storeys increases the safety level of the structure, while on the contrary the presence of soft storey involves strong uncertainties in terms of structural safety. Anyway, in the case-study under examination, for all the three limit states (NC, SD, DL), seismic demand results lower than the capacity and the verification is thence positive for all models (Fig. 11).

Particular attention was addressed to the distribution of the storey displacements and interstorey drifts, which allow to account for strength and stiffness discontinuities, so furnishing useful information on the damage that can be sustained by a building, including also non-structural elements. For the proposed case-study, storey displacements and interstorey drifts are plotted in Figs. 12a,b, for all models and for pushover run 1b in the *x* direction, with reference to the step corresponding to a fixed value of the base shear force (6000 kN). It emerges that the presence of infills leads to a significant diminution of the horizontal displacements, as a natural consequence of the increased stiffening. According to the previous considerations, a reduction of displacements is observed passing from the bare structure to the models with infills and soft storey and successively to the structures with infills in all storeys. It is interesting observing that in models C.1 and C.2 the interstorey drifts between the first and the second levels are higher than the ones in models B.1 and B.2, showing how in the case of infills in all storeys (B) the risk of formation of a storey soft mechanism at the 1st level is reduced with respect to the other models (A and C). Anyway there is no a substantial difference between single and double strut models.

Similar conclusions can be achieved by observing the collapse mechanisms of frames B.1, B.2 and C.1, C.2. In all cases, by monitoring the progressive development of the plastic hinges, the values of rotations corresponding to the ultimate bending moments are firstly reached at the base of the first-level columns and successively at the top of the second-level columns and at the extremities of the first-level beams. In the

same way in the equivalent struts the ultimate values of axial deformations are firstly reached at the first level and then at the second one. This means that a flexural collapse mechanism mainly involving the first two levels occurs (Fig. 13). Focusing on the behaviour of panels, with reference to models B.1 and B.2, Table 7, for each level, shows the number of panels in which the yield (F_y), critical (F_m) and residual (F_r) strength conditions are reached at the four steps of the pushover procedure corresponding, on the capacity curve, to the SD, NC, peak and last points, respectively. In both cases of single and double strut models, at the step corresponding to the NC limit condition, no panels have reached the critical strength, proving that masonry elements behave as strong infills, that is the increase brought to the overall strength and stiffness of the structure is active until high displacement ranges.

The choice of the infill macro-model contrarily significantly affects the structural response in terms of shear forces. Figure 14 illustrates for each model the shear time-histories at the end/critical sections of a column and a beam of the first level; in the same plots also the steps corresponding to the NC limit states and the value of the shear resistance related to a prescribed transversal reinforcement ratio are reported. More precisely the minimum area of shear reinforcement prescribed for critical regions in Medium Ductility Class, according to Eurocode 8 [8], is considered.

By observing Fig. 14a, regarding the end sections of a column of the first level, it emerges that shear values are lower than the shear resistance in all models except for the B.2 one; in this case, at the top end section of the column, the shear resistance is exceeded before the reaching of the NC limit state for bending. Similarly Fig. 14b, referring to a beam of the first level, shows that shear values are always lower than the shear resistance except for model C.2; also in this case, at the extremity of the beam, shear failure precedes the step corresponding to the NC limit state.

From the above results, it can be deduced that local response can be conveniently represented only by the double-strut model that, differently from the single-strut and the bare ones, is able to reproduce the considerable increase of shear in critical sections nearby the beam-column nodes due to the infill-frame interaction (Fig. 15). The most dangerous values of shear occur in columns, in proximity of structural nodes. As to beams, critical values are obtained especially at the soft storey level; in absence of soft storey, the highest values of shear force arise at the first level, at the extremities of each beam and at the intersection with the equivalent struts (Fig. 15b). As a consequence, by adopting the double strut model, in many cases the steps corresponding to the shear failures of columns or beams precede the steps associated to the NC

seismic performance level, clearly showing that shear local verifications are not satisfied. On the contrary bare and single-strut models are unable to reproduce these effects, leading to unsafe predictions since shear local verifications often result fully satisfied in critical regions.

In order to investigate the influence of the local shear interaction effects on the collapse mechanisms, pushover analysis of model B.2 was repeated by placing shear hinges at the nodal end sections of columns and beams in contact with infill panels, as described in section 3.1. The corresponding pushover curve in the *x* direction is reported in Fig. 16; it is evident a significant drop of resistance and ductility. By observing the plastic hinges formation sequence, it emerges that ultimate limit values of shear forces are first reached in most of the columns of the first level and successively in some columns of the second one, till the analysis stops. Bending hinges in columns and beams as well as axial hinges in equivalent struts never reach the ultimate condition. Figure 17 shows the deformed shape and the plastic-hinge configuration corresponding to the last step. It is clear that the formation of a brittle storey mechanism occurs at the first level. This result not only proves that the panel-frame interaction can substantially change the collapse mechanism of a structure under seismic action but also outlines how very dangerous failure modes can be omitted by ignoring the infill-frame interaction.

5 CONCLUSIONS

In this paper a study on the local shear effects produced at the ends of beams and columns of infilled RC buildings by the panel-frame interaction in the presence of lateral load has been presented. The main goal was to provide a practical tool in order to carry out reliable non-linear static analyses of RC frames taking into account the local interaction between panel and RC frame. At this purpose a comparison was carried out between the force arising in the frame members in the case of infills modeled as equivalent single-struts, according to the codes in force, and the ones arising in the case of infills modeled as equivalent double-struts, according to a new approach consisting in positioning the extremities of the two struts in correspondence of the points of application of the stress resultants on each side of the panel. All the theoretical and computational choices dealing with the structural modeling and the pushover procedure were accurately described, from the definition of the geometrical and mechanical properties of the equivalent struts to the correct identification of plastic hinge constitutive laws.

The results show that, by adopting the double-strut model, it is possible to capture dangerous local shear failures which can substantially change the collapse mechanism and that if neglected can lead to improper

and unsafe predictions of the seismic performance level of a RC framed building. In this framework the double-strut approach may represent an effective predictive tool for the accurate evaluation of frame-infill interaction effects in pushover analysis, since it could be easily implemented in commercial codes and could be applied for each dimension of panel frames.

REFERENCES

[1] Mainstone RJ. On the stiffness and strength of infilled frames. Proc Inst Civil Eng, Suppl (IV) – Lond 1971; Paper 7360S:57–89.

[2] Fardis MN. Experimental and numerical investigations on the seismic response of RC infilled frames and recommendations for code provisions. ECOEST/PREC 8, Rep. No. 6. LNEC. Lisbon; 1996.

[3] Klingner RE, Bertero VV. Earthquake resistance of infilled frames. J Struct Div 1978; 104(ST6):973–89.

[4] Dolsek M, Fajfar P. Soft storey effects in uniformly infilled reinforced concrete frames. J Earthq Eng 2001; 5(1):1–12.

[5] Verderame GM, De Luca F, Ricci P, Manfredi G. Preliminary analysis of a softstorey mechanism after the 2009 L'Aquila earthquake. Earthq Eng Struct D 2011; 40(8):925–44.

[6] Cavaleri L, Di Trapani F. Prediction of the additional shear action on frame members due to infills. B Earthq Eng 2014, DOI: 10.1007/s10518-014-9668-z.

[7] FEMA 356. Prestandard and commentary for the seismic rehabilitation of buildings; 2000.

[8] CEN. Eurocode 8: design of structures for earthquake resistance. Part 1: general rules, seismic actions and rules for buildings. Brussels; 2005.

[9] DM 14/01/2008. Norme Tecniche per le Costruzioni. Gazzetta Ufficiale n.29. Roma; 2008 [in Italian].

[10] Polyakov SV. On the interaction between masonry filler walls and enclosing frame when loaded in plane of the wall. Earthquake Engineering 1960. Earthquake Research Institute. San Francisco.

[11] Amato G, Fossetti M, Cavaleri L, Papia M. An updated model of equivalent diagonal strut for infill panels. Eurocode 8 perspectives from Italian standpoint, workshop; 2008. p. 119–28.

[12] Crisafulli FJ, Carr AJ, Park R. Analytical modelling of infilled frames structures – a general review. Bull NZ Soc Earthq Eng 2000; 33(1):30–47.

[13] Hak, S., Morandi, P. & Magenes, G. Local effects in the seismic design of RC frame structures with masonry infills. 4th ECCOMAS Thematic Conference on Computational Methods in Structural Dynamics and Earthquake Engineering, Kos Island, 2013.

[14] Asteris PG, Antoniou ST, Sophianopoulos DS, Chrysostomou CZ. Mathematical macromodeling of infilled frames: state of the art. J Struct Eng ASCE 2011; 137(12):1508–1517.

[15] Chrysostomou CZ, Asteris PG. On the in-plane properties and capacities of infilled frames. Eng Struct 2012; 41:385–402.

[16] Crisafulli FJ, Carr AJ, Park R. Analytical modelling of infilled frames structures: a general review. Bull N Z Soc Earth Eng 2000; 33(1):30–44.

[17] Crisafulli FJ, Carr AJ. Proposed macro-model for the analysis of infilled frame structures. Bull N Z Soc Earth Eng 2007; 40(2):69–77.

[18] El-Dakhakhni W, Elgaaly M, Hamid A. Three-Strut Model for Concrete Masonry-Infilled Steel Frames. J Struct Eng (ASCE) 2003; 192(2):177-185.

[19] Chrysostomou CZ, Gergely P, Abel JF. A six-strut model for nonlinear dynamic analysis of steel infilled frames. Int J Struct Stab Dy 2002; 2(3):335-353.

[20] Liauw TC and Lee SW. On the behavior and analysis of multi-storey infilled frames subject to lateral loads. Proc. of the ICE, Part 2, 1977, 641-656.

[21] Campione G, Cavaleri L, Macaluso G, Amato G, Di Trapani F. Evaluation of infilled frames: an updated in-plane-stiffness macro-model considering the effects of vertical loads. B Earthq Eng 2014; DOI 10.1007/s10518-014-9714-x.

[22] Asteris PG, Cavaleri L, Di Trapani F & Sarhosis V. A macromodelling approach for the analysis of infilled frame structures considering the effects of openings and vertical loads, Struct Infrastruct E 2015, DOI: 10.1080/15732479.2015.1030761.

[23] Cavaleri L, Papia M. A new dynamic identification technique: application to the evaluation of the equivalent strut for infilled frames. Eng Struct 2003; 25:889–901

[24] Di Trapani F, Macaluso G, Cavaleri L, Papia M. Masonry infills and RC frames interaction: literature overview and state of the art of macromodeling approach. Eur J Environ Civ En 2015. DOI: 10.1080/19648189.2014.996671.

[25] Cavaleri L, Di Trapani F. Cyclic response of masonry infilled RC frames: Experimental results and simplified modelling. Soil Dyn Earthq Eng 2014; 65:224-242.

[26] Fiore A, Netti A, Monaco P. The influence of masonry infill on the seismic behaviour of RC frame buildings. Eng Struct 2012; 44:133-145.

[27] El-Dakhakhni W, Hamid A., Elgaaly M. Strength and stiffness prediction of masonry infill panels. 13th World Conference on Earthquake Engineering 2004; Vancouver, B.C. Canada, August 1-6 2004, Paper No. 3089.

[28] Holmes M. Steel frames with brickwork and concrete infilling. Proc Inst Civil Eng, Part 2, Lond 1981;19:473–8.

[29] Paulay T, Priestley MJN. Seismic design of reinforced concrete and masonry buildings. New York: John Wiley & Sons; 1992.

[30] Penelis GG, Kappos AJ. Earthquake-resistant concrete structures. London: E &FN Spon; 1997.

[31] M.L.P. Circolare 10 Aprile 1997, Istruzioni per l'applicazione delle norme tecniche per le costruzioni in zone sismiche di cui al decreto ministeriale 16 gennaio 1996. Supplemento Ordinario alla Gazzetta Ufficiale n. 97, Ministero dei Lavori Pubblici; 1997.

[32] Stafford Smith B. Behaviour of square infilled frames. J Struct Div 1966; 92(1):381–403.

[33] Klingner RE, Bertero VV. Infilled frames in earthquake-resistant construction. Report EERC 76-32. Earthquake Engineering Research Center; 1976.

[34] Bertoldi SH, Decanini LD, Gavarini C. Telai tamponati soggetti ad azioni sismiche, un modello semplificato: confronto sperimentale e numerico. Atti del 6 Convegno Nazionale ANIDIS, vol. 2, Perugia, 13–15 Ottobre 1993 [in Italian]. p. 815–24.

[35] Papia M, Cavaleri L, Fossetti M. Infilled frames: developments in the evaluation of the stiffening effect of infills. Struct Eng Mech 2003; 16.

[36] Panagiotakos TB, Fardis MN. Seismic response of infilled RC frames structures. In: Proceedings of 11th world conference on earthquake engineering. Acapulco; 1996 [Paper No. 225].

[37] Cavaleri L, Di Trapani F, Papia M. Strutture intelaiate in c.a. con tamponamenti: analisi degli effetti locali in presenza di azioni sismiche. XV Convegno ANIDIS. L'Ingegneria Sismica in Italia, 30 Giugno – 4 Luglio 2013, Padova [in Italian].

[38] CEN (2001). Eurocode 2. Design of concrete structures - Part 1: General rules and rules for buildings. EN 1992-1.

[39] Fardis MN, Carvalho EC, Fajfar P, Pecker A. Seismic Design of Concrete buildings to Eurocode 8; CRC Press, Taylor & Francis Group, 2015.

[40] Fajfar P, Gaspersic P. The N2 method for the seismic damage analysis of RC buildings. Earthq Eng Struct D 1996; 28: 979–93.

[41] Fiore A and Monaco P. Earthquake-induced pounding between the main buildings of the "Quinto Orazio Flacco" school. Earthq Struct 2010; 1(4): 371-390.

[42] Fiore A, Monaco P. Analysis of the seismic vulnerability of the ‘‘Quinto Orazio Flacco’’ school in Bari (Italy) [Analisi della vulnerabilità sismica del Liceo ‘‘Quinto Orazio Flacco’’, Bari]. Ingegneria Sismica 2011; 28(1): 43–62.

[43] Magenes G, Della Fontana A. Verifica di edifici in muratura ordinaria e armata con metodi di analisi statica, lineare e non lineare. ANPEL, Alecom srl, 2010 [in italian].

List of Figure captions

Figure 1. Transmission of forces from the masonry panel to the surrounding reinforced concrete frame under seismic actions.

Figure 2. Infill panel macro-models: *a*) single strut model; *b*) double strut model.

Figure 3. Bertoldi et al. [34] constitutive law.

Figure 4. a) Bertoldi et al. constituve laws for four failure modes; b) comparison between the constitutive laws of Panagiotakos et al., Bertoldi et al. (second collapse mode σ_{w2}) and Cavaleri et al. for the infill panel P_{X01}.

Figure 5. The case study: a) typical structural plan; b) Section in the *y* direction.

Figure 6. The case study. Sections and reinforcements of: a) beams; b) columns; c) floors at the generic level (1) and at the top level (2) (dimensions in mm).

Figure 7. Finite element models: a) Mod A, b) Mod B.2, c) Mod C.1.

Figure 8. a) Moment-Rotation relationship of frame element plastic hinges; b) Force-Displacement relationship of equivalent strut plastic hinges; c) Shear-Displacement relationship of frame element plastic hinges.

Figure 9. Natural vibration periods of the first six mode shapes for all models.

Figure 10 a) Mod B.2, Push 1b), *x* direction: variation of the capacity curve in function of E_{90}; b) variation of the Bertoldi et al. constitutive law (second collapse mode σ_{w2}) in function of E_{90} for the infill panel P_{X01}.

Figure 11. Push 1b), pushover curves for all models: a) *x* direction; b) *y* direction.

Figure 12. PUSH 1b), *x* direction, step corresponding to a value of the base shear force equal to 6000 kN : a) storey displacements; b) interstorey drifts.

Figure 13. Plastic hinge configuration, Push 1b), *x* direction, model B.1, last step.

Figure 14. Shear time-histories and resistance verifications, Push 1b), *x* Direction. a) column 30x80 cm^2, first level, critical region Φ8/14 cm; b) beam 30x60 cm^2, first level, critical region Φ8/13 cm

Figure 15. Shear diagrams in the *x* direction, Push 1b), steps corresponding to the NC performance level: a) Mod B.1; b) Mod B.2.

Figure 16. Push 1b), x direction: comparison between pushover curves with and without including shear hinges.

Figure 17. Pushover run with shear hinges in columns and beams: plastic hinge configuration, Push 1b), *x* direction, model B.2, last step.

List of Table captions

Table 1. Different formulations for the calculus of the width b_w of equivalent struts.

Table 2. Determination of parameters K_1 and K_2 [34].

Table 3. Mechanical properties of concrete and steel.

Table 4. Mechanical and geometrical properties of infill panels.

Table 5. Seismic hazard parameters of the site.

Table 6. Global stiffness percentage-increments of infilled structures with respect to the bare model.

Table 7. Number of panels in which the yield (F_y), critical (F_m) and residual (F_r) strength conditions are reached at four steps of the pushover procedure (SD, NC, peak and last points) for Models B.1 and B.2

Table 1

Click here to download Table: Table_1.docx

Method	Circ. 10/04/1997	Holmes	Stafford-Smith	Klingner & Bertero	Papia
Panel	$b_w=0.10d$	$b_w=0.33d$	$b_w=(\pi/\lambda)\sin\theta$	$b_w=0.175d\,(\lambda h')^{-0.4}$	$b_w=d\,(c/z)(\lambda^*)^{-\beta}$
P_{X01}	0.60	1.97	2.74	0.67	1.67
P_{X02}	0.58	1.91	3.29	0.69	1.67
P_{X03}	0.53	1.75	2.10	0.66	1.43
P_{X04}	0.51	1.68	2.55	0.67	1.42
P_{Y01}	0.64	2.11	2.75	0.73	1.77
P_{Y02}	0.64	2.13	2.94	0.77	1.80
P_{Y03}	0.58	1.91	2.08	0.74	1.51
P_{Y04}	0.58	1.92	2.27	0.77	1.53

d=diagonal length of the panel; $\lambda = \sqrt[4]{\frac{E_w t_w \sin 2\theta}{4E_c I_P h}}$; E_w = elastic modulus of the infill panel; E_c=elastic modulus of the RC frame; I_P = moment of inertia of the column; t_w =thickness of the panel; h = height of the panel; θ =slope of the infill diagonal; c =0.249 – 0.0116ν+0.567 ν^2; β =0.146 - 0.0073ν+0.126 ν^2; $1 \le z \le 1.125$; ν=Poisson's coefficient of the infill along the diagonal direction; $\lambda^* = \frac{E_{w\theta}}{E_c}\frac{t_w h'}{A_C}\left(\frac{h'^2}{l'^2} + 0.25\frac{A_C}{A_B}\frac{l'}{h'}\right)$; $E_{w\theta}$ =elastic modulus of masonry evaluated along the diagonal; A_C=transversal area of the adjacent columns; A_B=transversal area of the upper beam; h'=height of the frame, measured between the centerlines of the beams; l' = length of the frame, measured between the centerlines of the columns.

Table 2

Click here to download Table: Table_2.docx

	$\lambda h < 3.14$	$3.14 < \lambda h < 7.85$	$\lambda h > 7.85$
K_1	1.3	0.707	0.47
K_2	-0.178	0.01	0.04

Table 3

Click here to download Table: Table_3.docx

Concrete			Steel		
R_{ck}	35	N/mm^2	f_{yk}	450	N/mm^2
f_{ctk}	1.94	N/mm^2	E_S	210000	N/mm^2
E_{cm}	32308	N/mm^2			

Table 4

Click here to download Table: Table_4_review 2.docx

Property			P_{X01}	P_{X02}	P_{X03}	P_{X04}	P_{Y01}	P_{Y02}	P_{Y03}	P_{Y04}
Direction	Ax. glob.	-	x	x	x	x	y	y	y	y
Storey level	-	-	1	1	2,3,4	2,3,4	1	1	2,3,4	2,3,4
Length	l	m	4.45	4.20	4.45	4.20	5.00	5.05	5.00	5.05
Heigth	h	m	4.00	4.00	2.90	2.90	4.00	4.00	2.90	2.90
Aspect ratio	l/h	-	1.11	1.05	1.53	1.45	1.25	1.26	1.72	1.74
Thickness	t_w	m	0.365	0.365	0.365	0.365	0.365	0.365	0.365	0.365
Diagonal length	d	m	5.98	5.80	5.31	5.10	5.98	5.80	5.31	5.10
Inclination	θ	rad	0.733	0.768	0.576	0.611	0.681	0.663	0.524	0.524
Diag. elastic modulus	E_w	Mpa	1000	1000	1000	1000	1000	1000	1000	1000
Elastic modulus parallel to bed joints	E_0	Mpa	825	825	825	825	825	825	825	825
Elastic modulus normal to bed joints	E_{90}	Mpa	1100	1100	1100	1100	1100	1100	1100	1100
Shear modulus	G	Mpa	400	400	400	400	400	400	400	400
Poisson ratio	ν	-	0.25	0.25	0.25	0.25	0.25	0.25	0.25	0.25

Table 5

Click here to download Table: Table_5.docx

	a_g/g	F_0	T^*_C (sec)	S_S	C_C	S_T
NC	0.217	2.594	0.494	1.175	1.267	1
SD	0.173	2.614	0.451	1.2	1.29	1
DL	0.079	2.582	0.354	1.2	1.354	1

Table 6

Click here to download Table: Table_6.docx

Model	Force Pattern	Stiffness variation [%]	
		x direction	*y* direction
Mod B.1	Push 1b)	64.8	54.4
	Push 2a)	63.7	55.6
Mod B.2	Push 1b)	78.8	64.2
	Push 2a)	74.1	62.8
Mod C.1	Push 1b)	13.9	6.0
	Push 2a)	7.2	2.7
Mod C.2	Push 1b)	14.6	6.0
	Push 2a)	7.2	2.7

Table 7

Click here to download Table: Table_7.docx

Model	capacity curve point	First level			Second level			Third level			Fourth level		
		F_y	F_m	F_r	F_y	F_m	F_r	F_y	F_m	F_r	F_y	F_m	F_r
Mod. B.1	SD	/	/	/	10	/	/	/	/	/	/	/	/
Mod. B.2	SD	/	/	/	10	/	/	/	/	/	/	/	/
Mod. B.1	NC	10	/	/	10	/	/	8	/	/	/	/	/
Mod. B.2	NC	10	/	/	10	/	/	2	/	/	/	/	/
Mod. B.1	peak point	10	10	/	10	10	/	10	/	/	/	/	/
Mod. B.2	peak point	10	10	/	10	10	/	10	/	/	/	/	/
Mod. B.1	last point	10	10	/	10	10	/	10	/	/	/	/	/
Mod. B.2	last point	10	10	/	10	10	/	10	/	/	/	/	/

Figure 1

Click here to download high resolution image

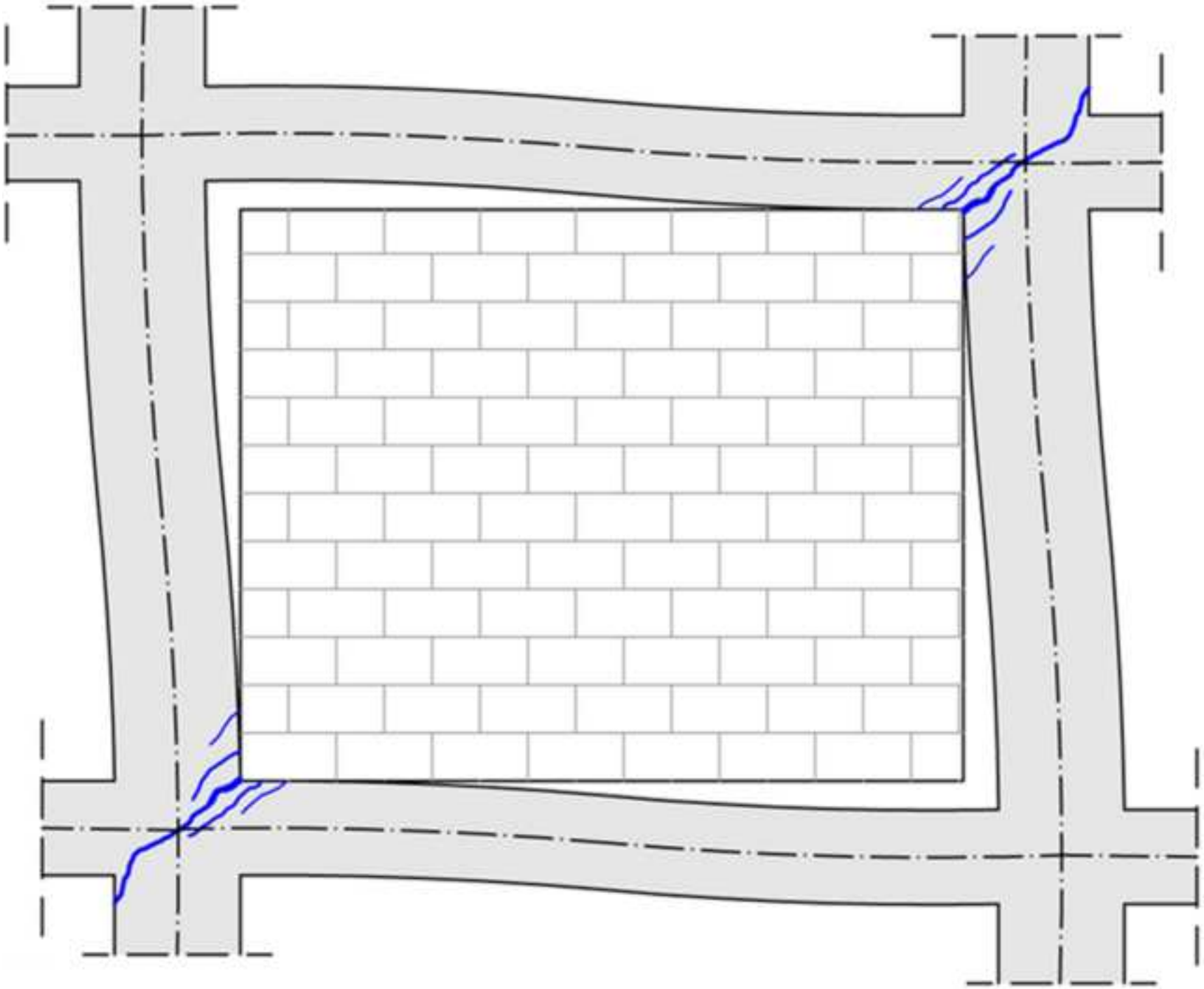

Figure 2

Click here to download high resolution image

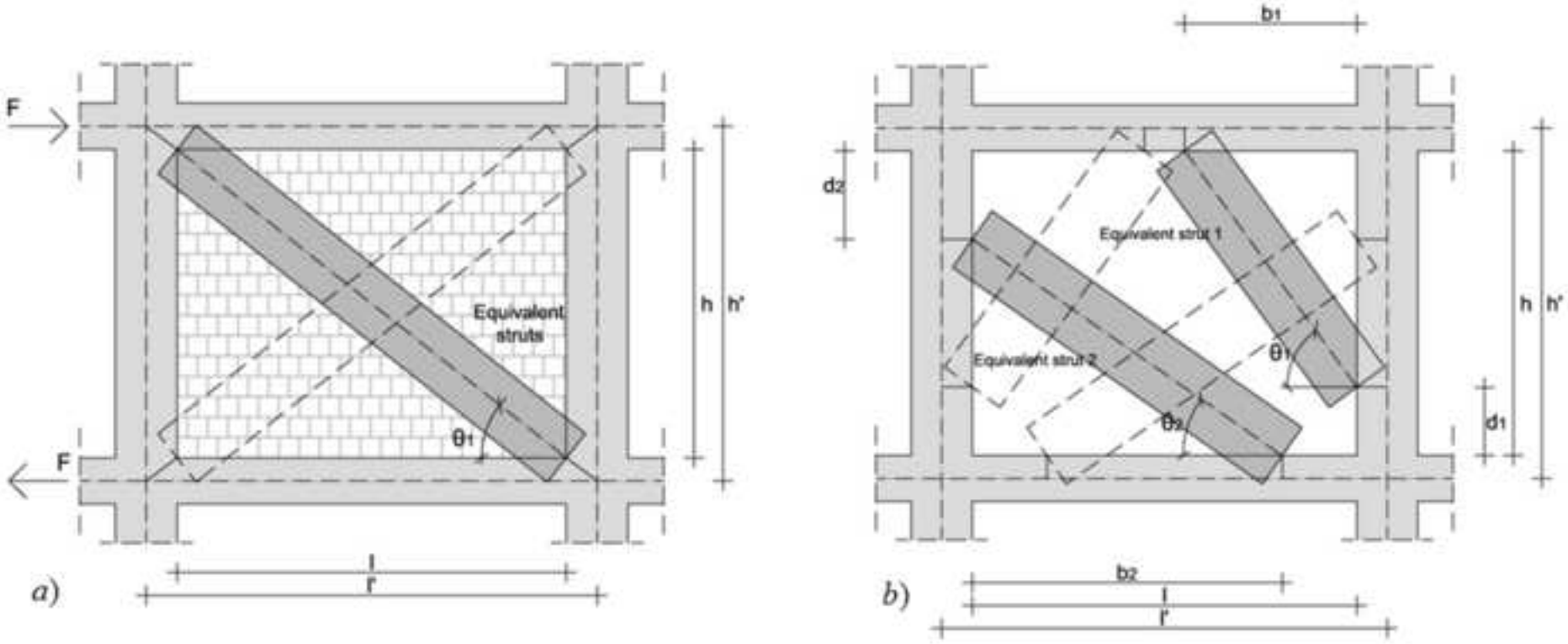

Figure 3

Click here to download high resolution image

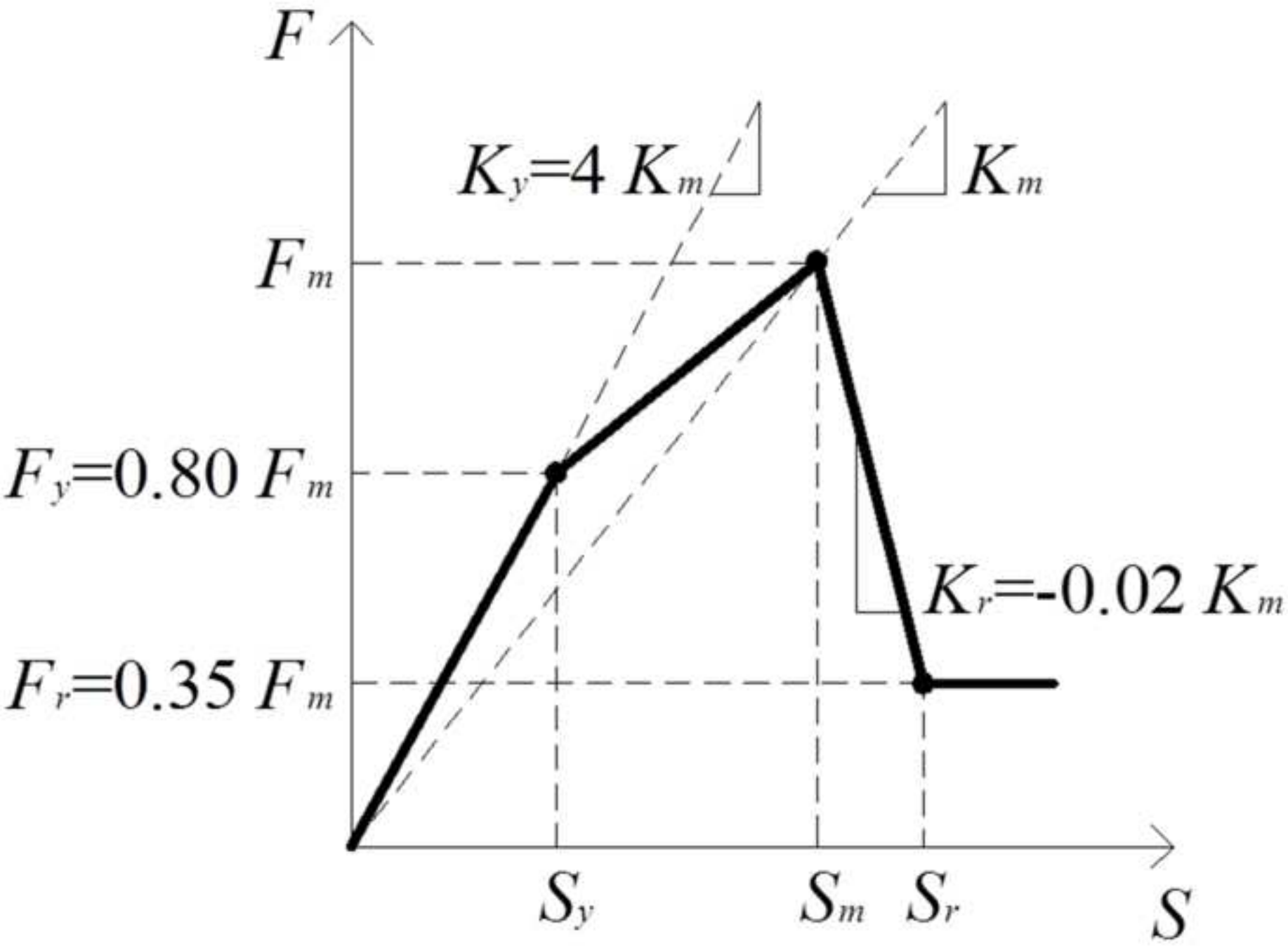

Figure 4

Click here to download high resolution image

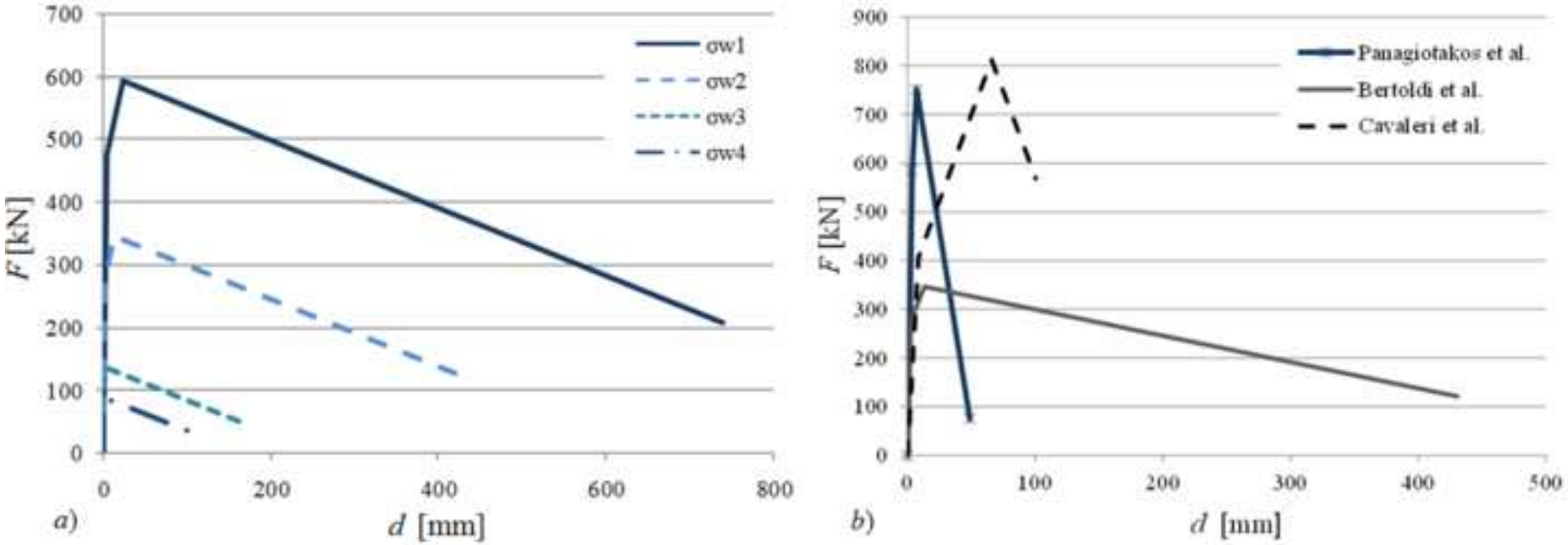

Figure 5

Click here to download high resolution image

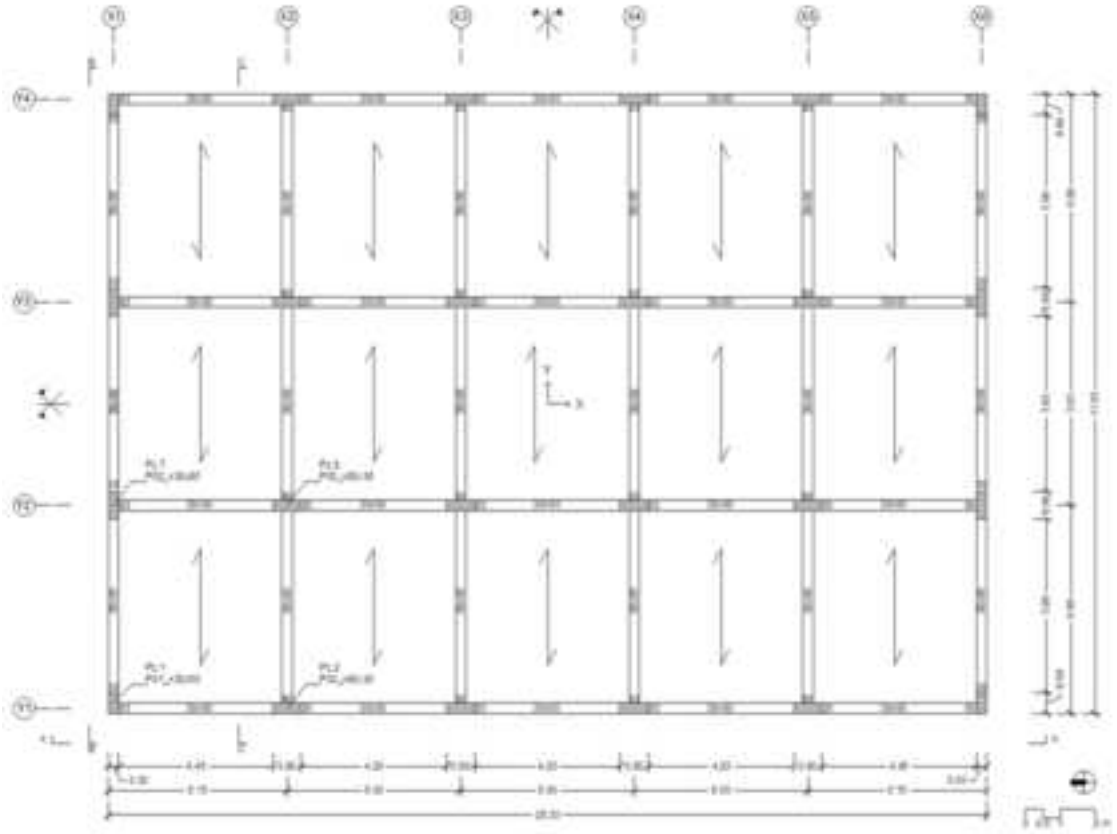

a)

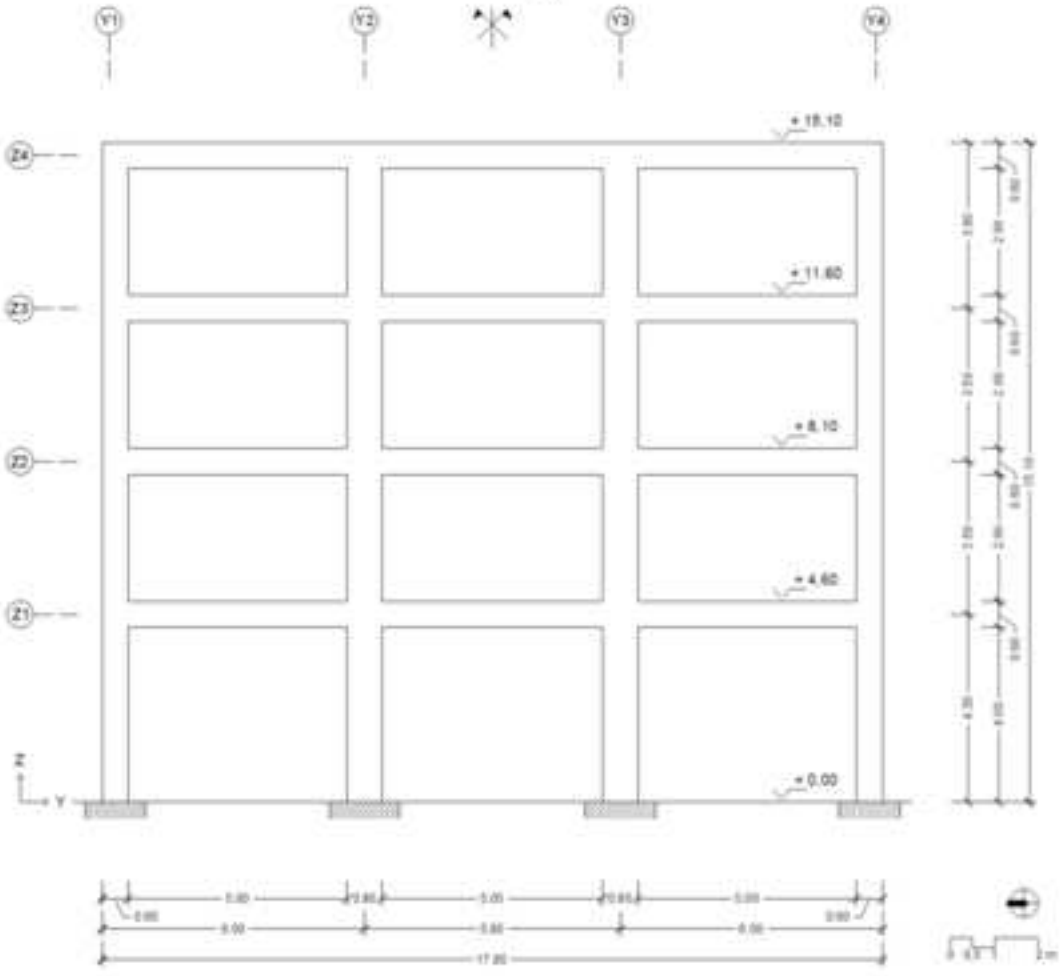

b)

Figure 6

Click here to download high resolution image

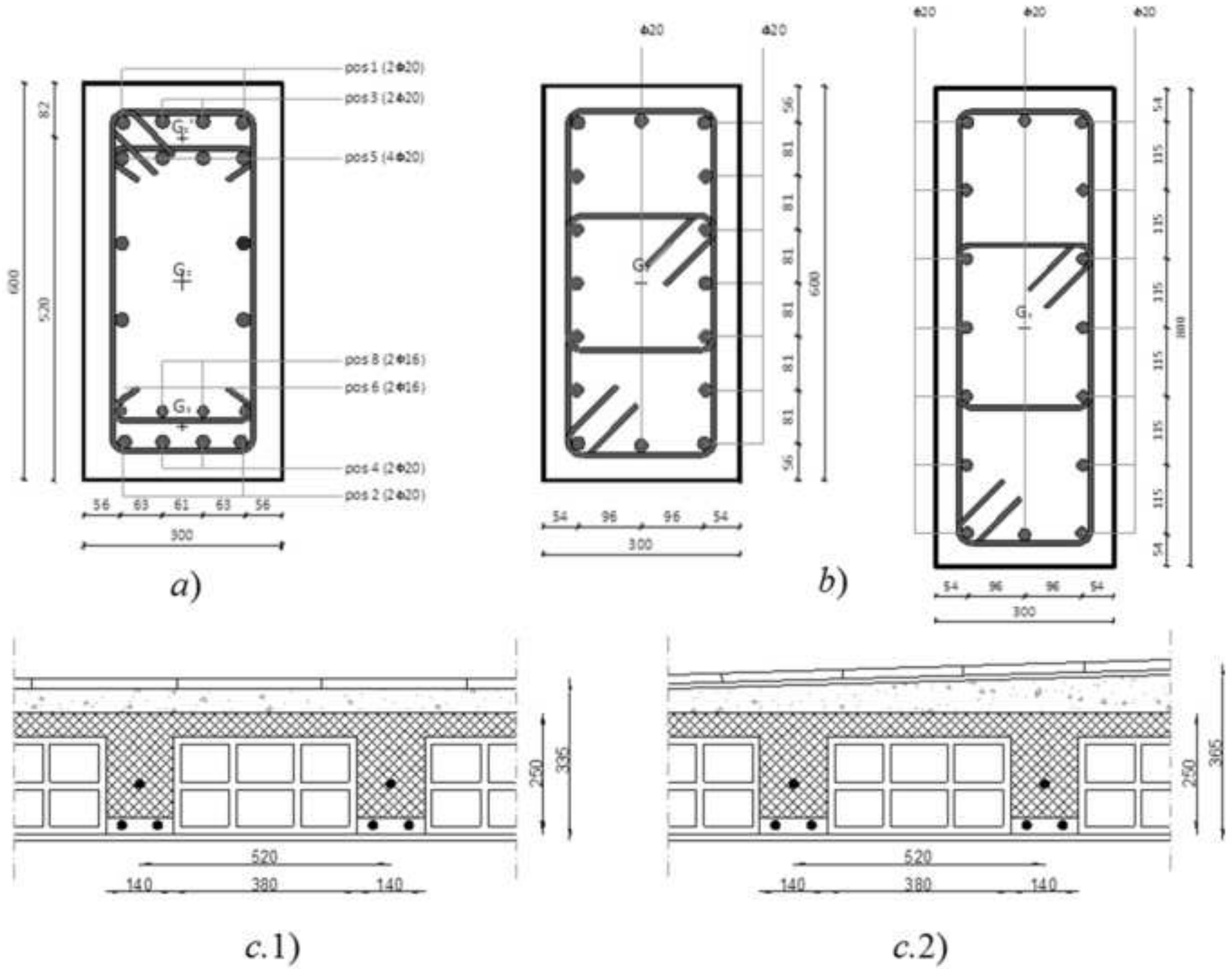

Figure 7

Click here to download high resolution image

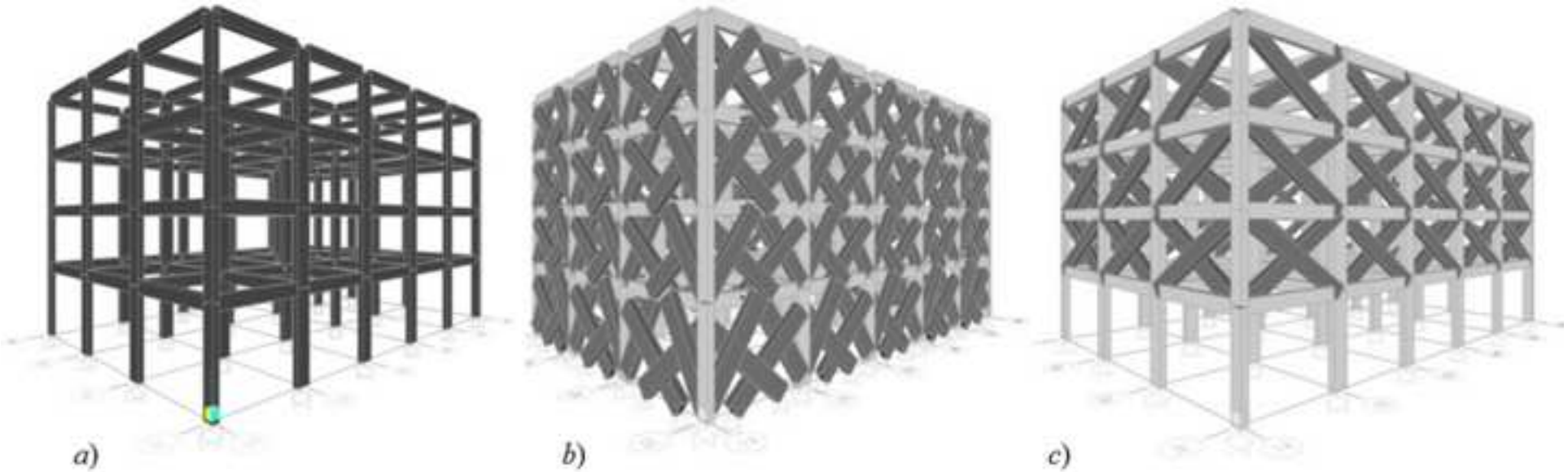

Figure 8

Click here to download high resolution image

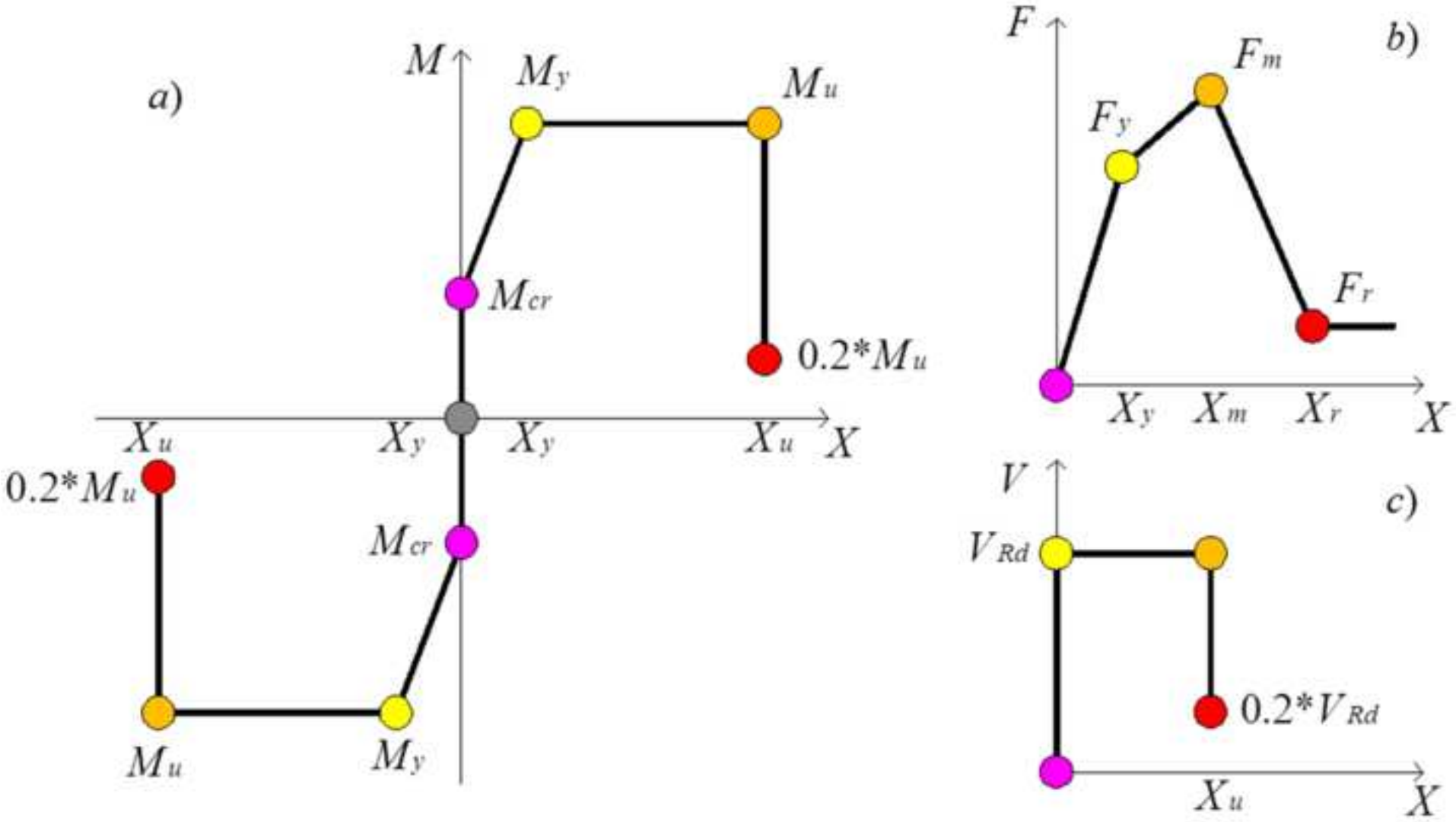

Figure 9

Click here to download high resolution image

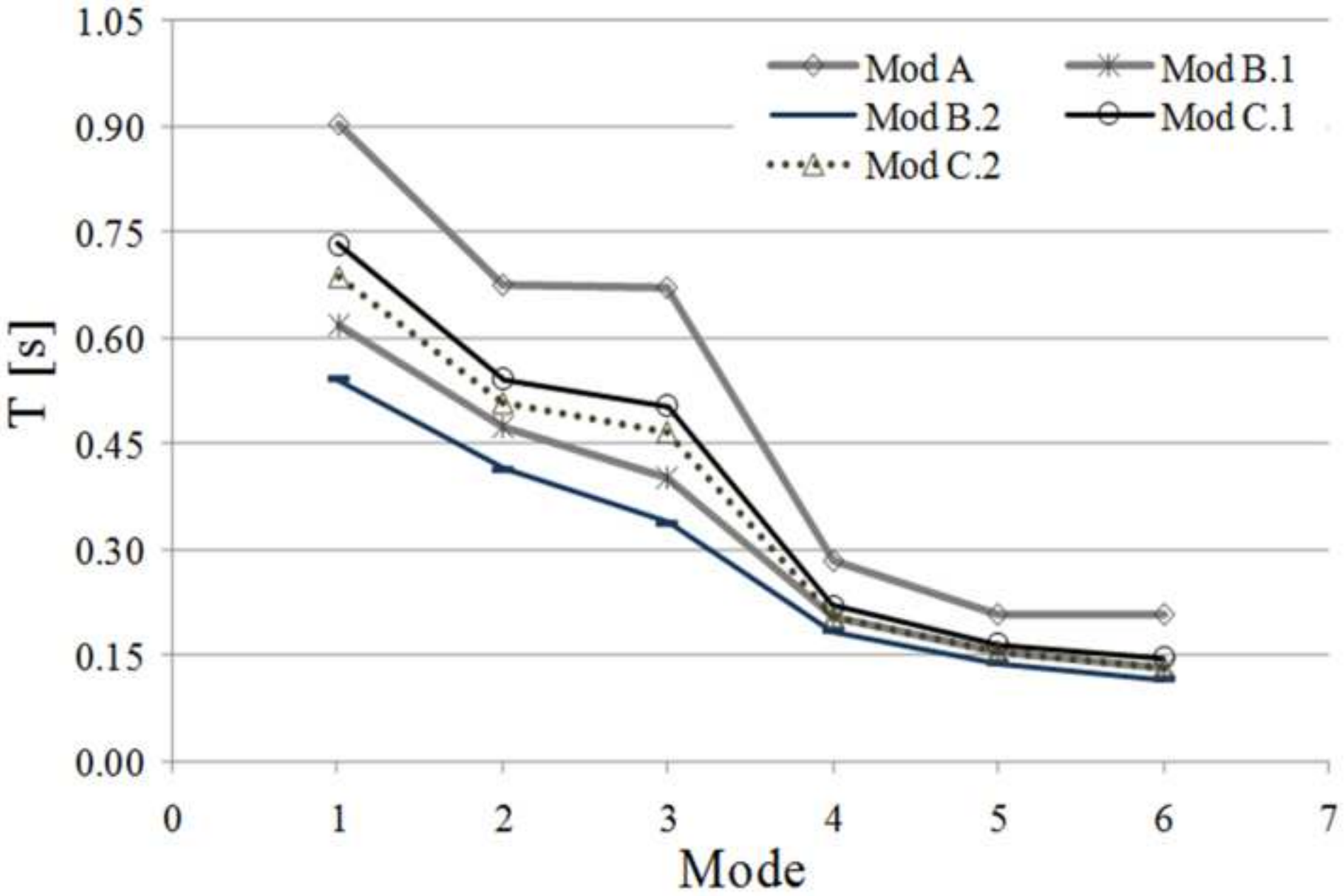

Figure 10

Click here to download high resolution image

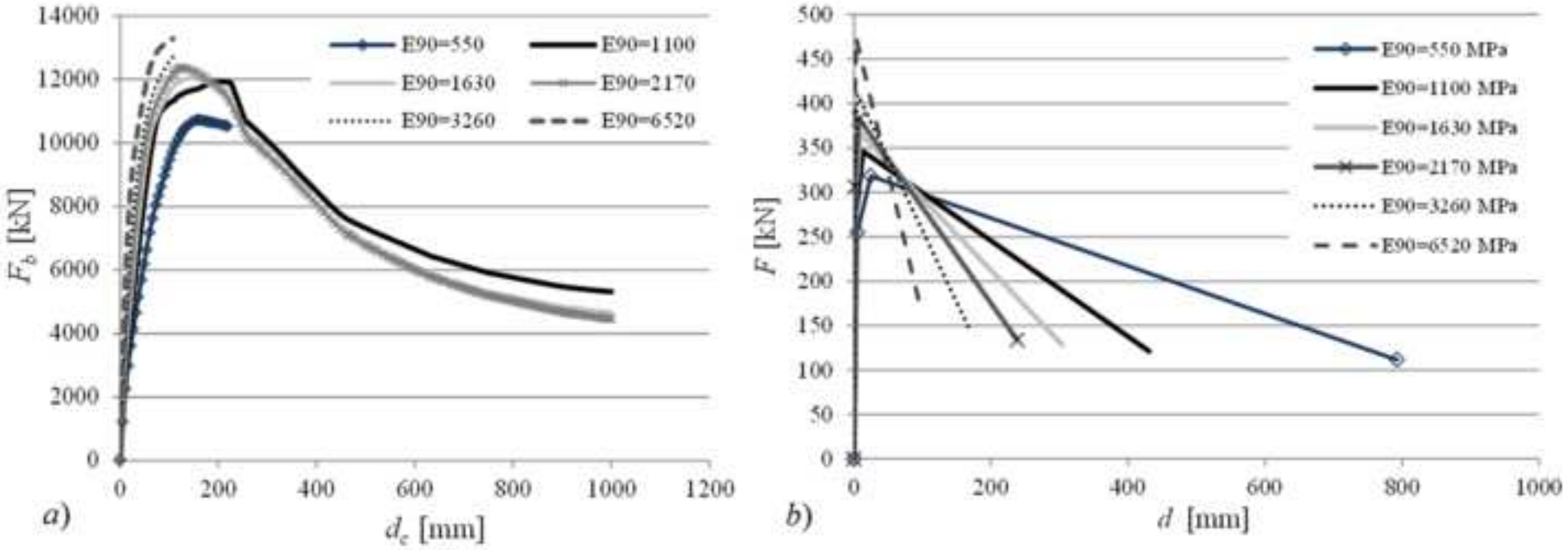

Figure 11

Click here to download high resolution image

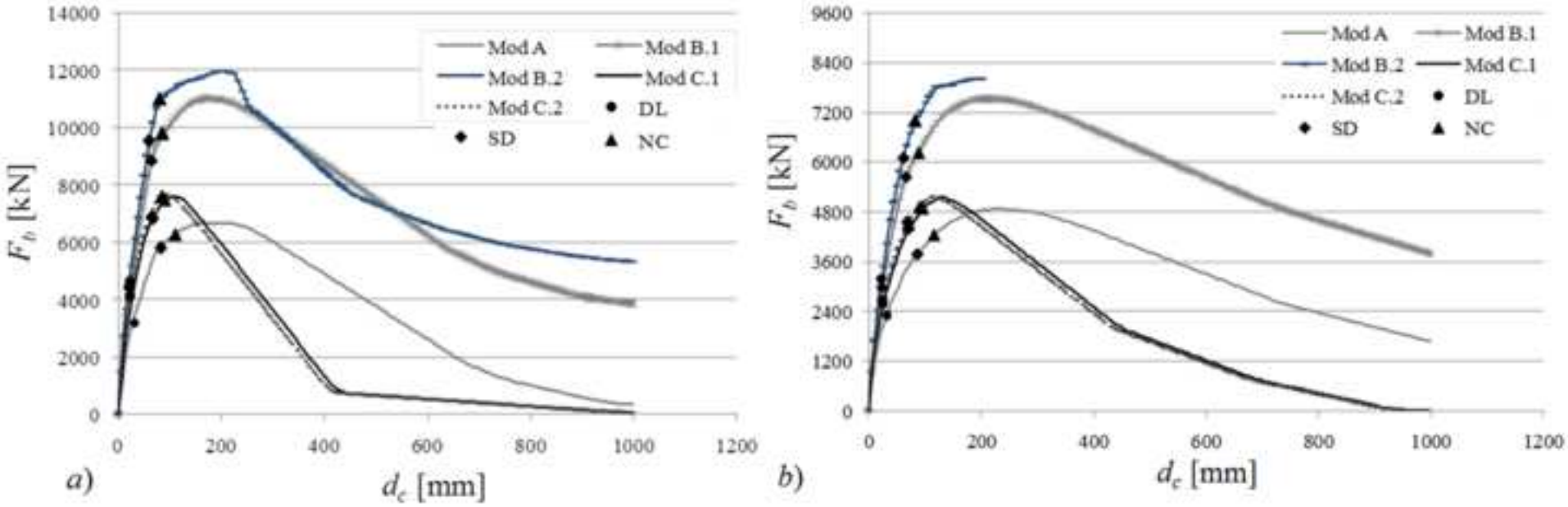

Figure 12

Click here to download high resolution image

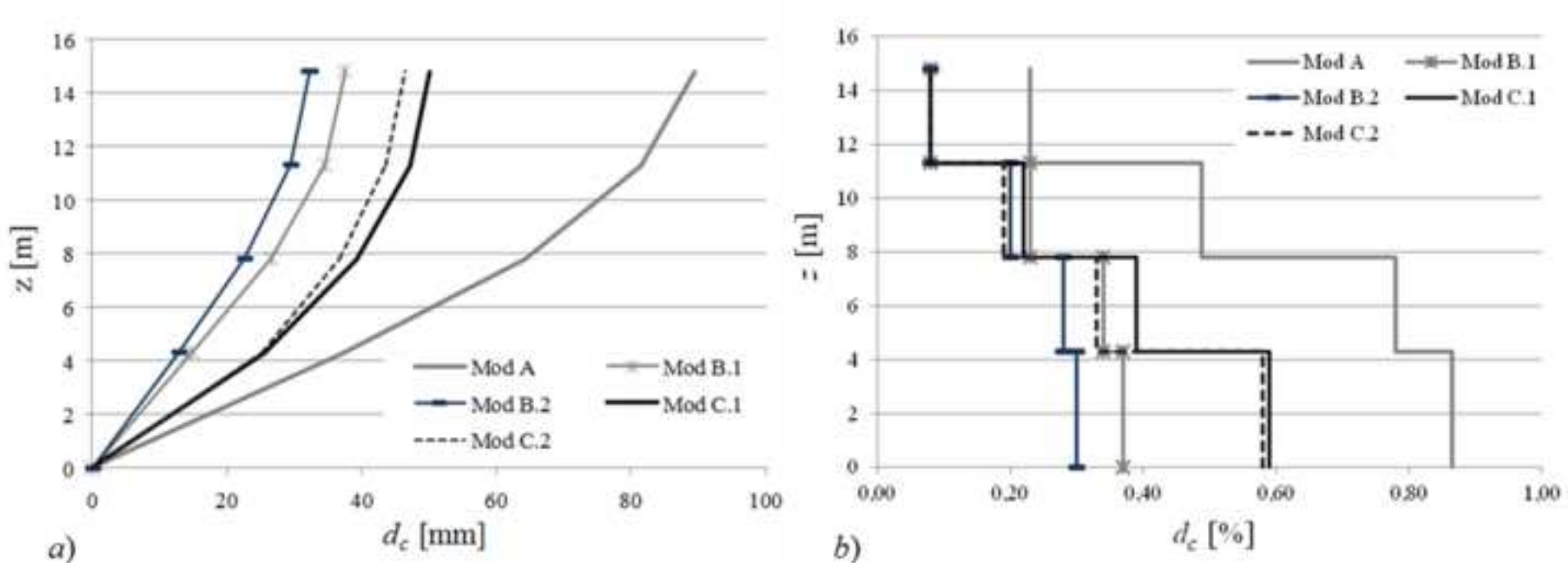

Figure 13

Click here to download high resolution image

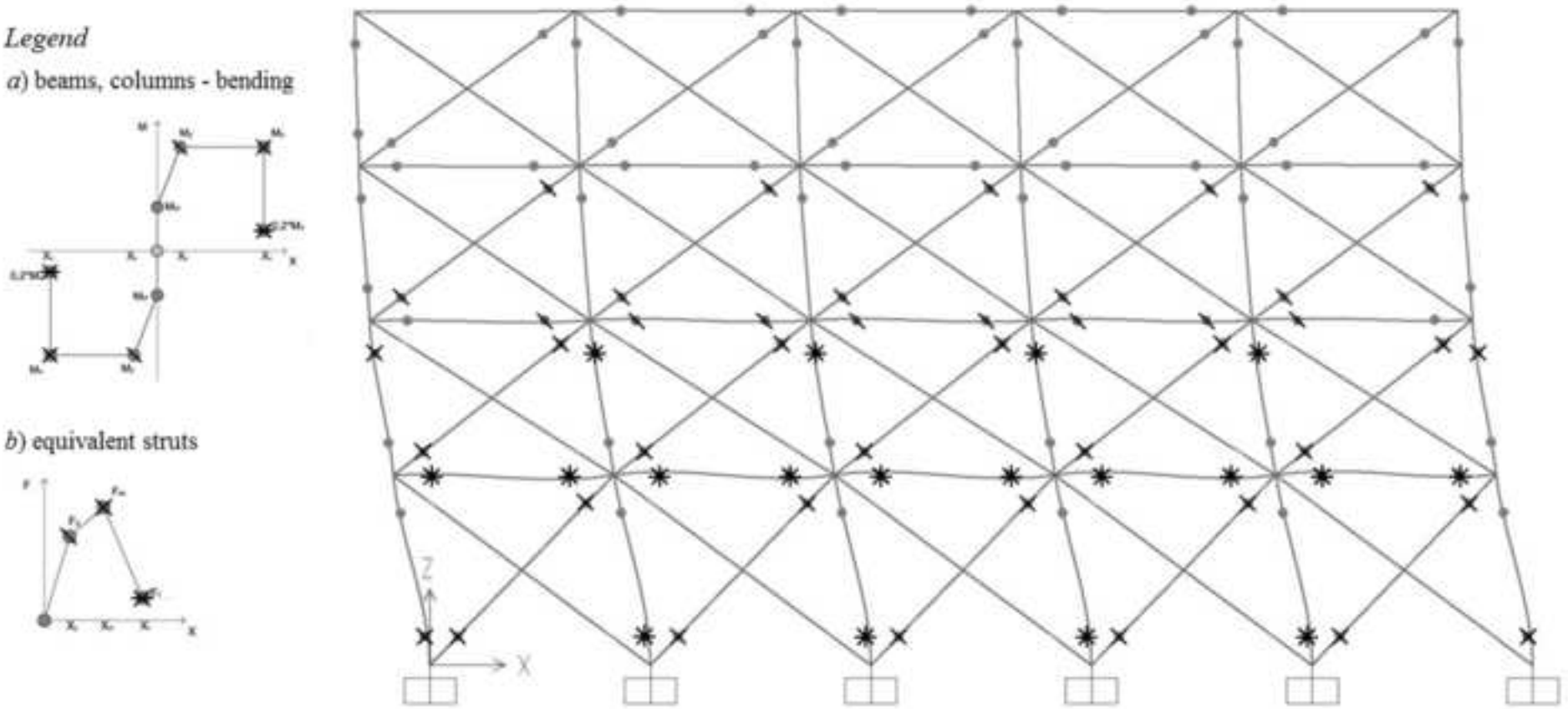

Figure 14

Click here to download high resolution image

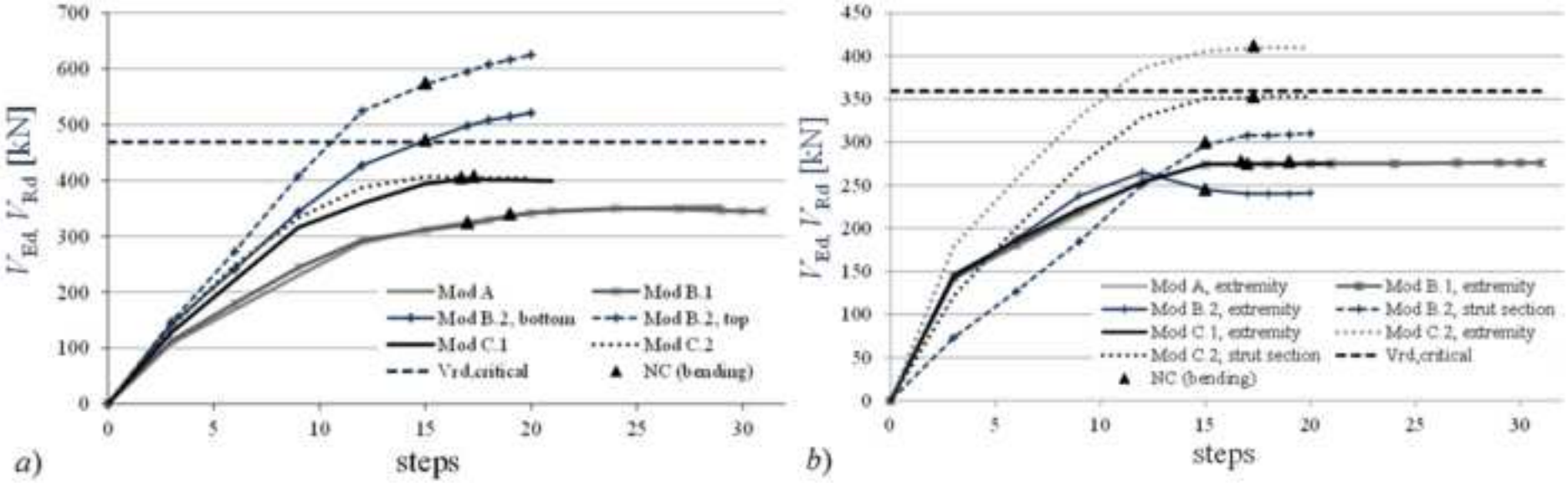

Figure 15
Click here to download high resolution image

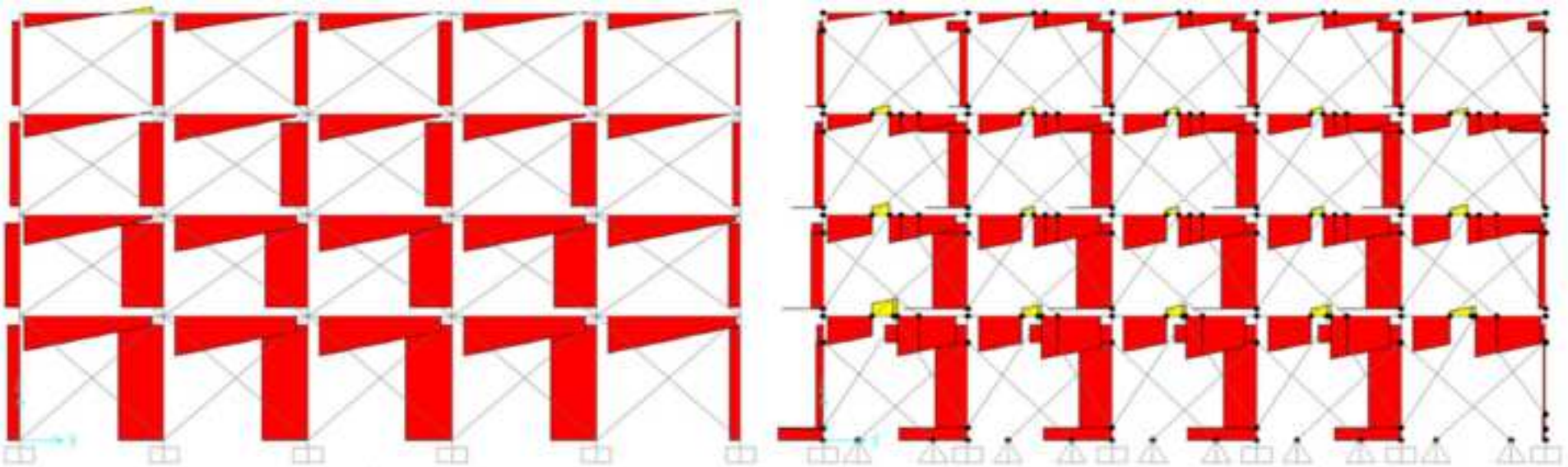

a) b)

Figure 16

Click here to download high resolution image

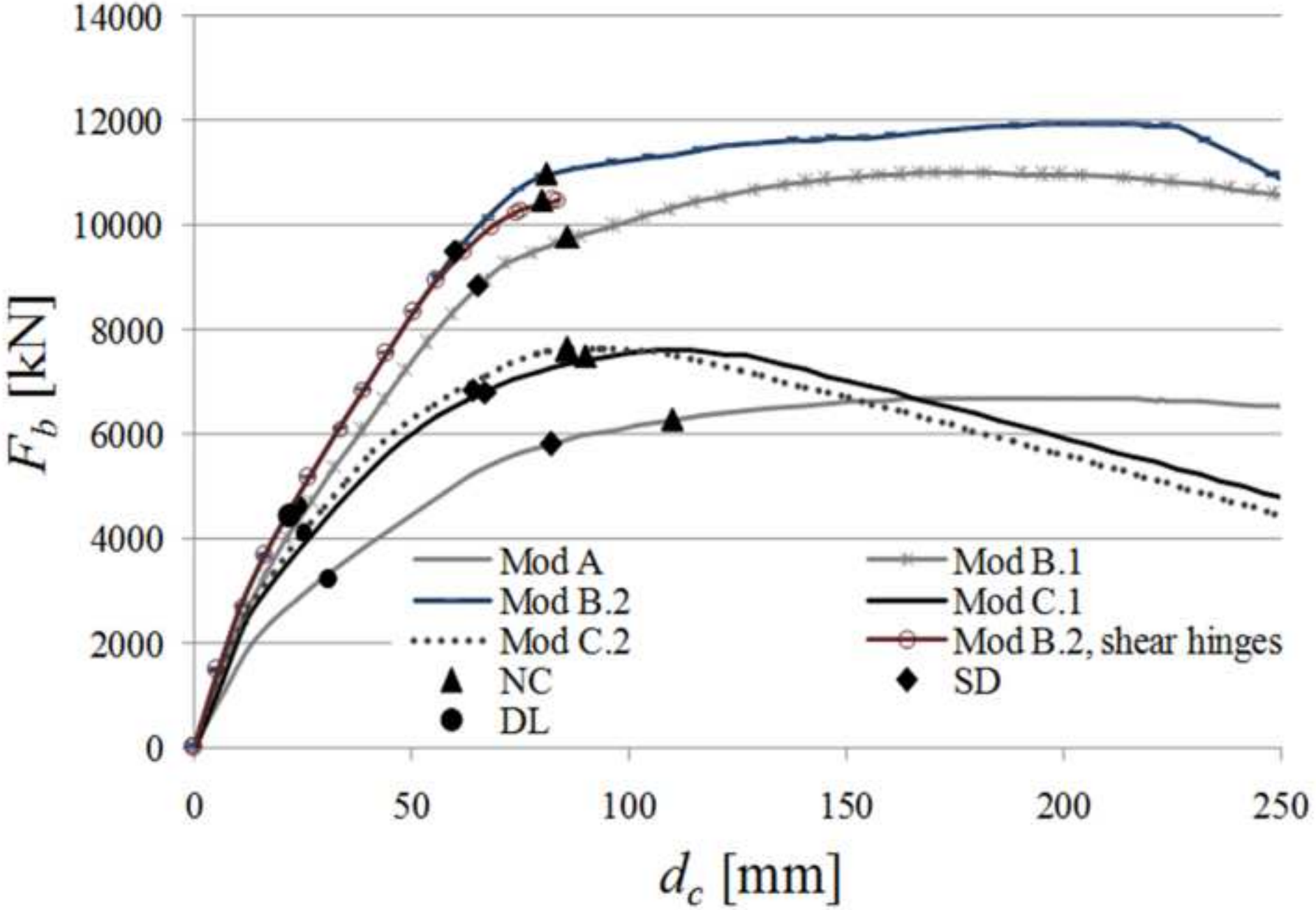

Figure 17

Click here to download high resolution image